Journal of the Korean Association of Crystal Growth
Vol. 11, No. 4 (2001) 170-175

Growth and characterization of Al_2O_3-based $Y_3Al_5O_{12}$, ZrO_2 binary and ternary eutectic fibers

J.H. Lee†, A. Yoshikawa, H. Kaiden, T. Fukuda, D.H. Yoon* and Y. Waku**

Institute for Materials Research, Tohoku University, Sendai 980-8577, Japan
**School of Metallurgical and Materials Eng., Sungkyunkwan Univ., Suwon 440-746, Korea*
***Japan Ultra-high Temperature Materials Research Center, Ube 755-0001, Japan*

(Received May 21, 2001)

Abstract It was possible to grow the Al_2O_3 based $Y_3Al_5O_{12}$ (YAG), ZrO_2 binary and ternary eutectic fibers using micro-pulling down method with a growing rate of 0.1~15 mm/min. While Al_2O_3/ZrO_2 showed cellular-lamellar structure, Al_2O_3/YAG and Al_2O_3/YAG/ZrO_2 ternary eutectic fibers showed homogeneous Chinese script lamellar structures. The microstructure of Al_2O_3/ZrO_2 binary eutectic fibers changed with solidification rate from lamellar pattern to cellular structure. The interlamellar spacing agreed with the inverse-square-root dependence on pulling rate according to $\lambda = kv_p^{-1/2}$. Al_2O_3/ZrO_2 binary eutectic fibers recorded the highest tensile strength of about 1560MPa at room temperature. Al_2O_3/YAG/ZrO_2 ternary eutectic fiber showed excellent thermal stability to 1200°C without significant decrease. The maximum strength of ternary eutectic fibers recorded were 1100MPa at 25°C and 970 MPa at 1200°C, respectively.

1. Introduction

In various industrial fields for example electric power plant and aerospace industries, there are strong needs for high temperature structural materials in order to increase the energy efficiency.

Directionally solidified ceramic eutectics are attracting considerable interest because of their high structural stability up to nearly the melting temperature [1]. Since early 1960s, systematic investigations of oxide eutectics began and considerable research has been devoted to the structure and properties of these eutectics.

A few years ago, promising results were reported for the Al_2O_3-based binary eutectic systems such as $Al_2O_3/GdAlO_3$ [1], $Al_2O_3/Y_3Al_5O_{12}$ (below abbreviated as YAG) [2-5] and Al_2O_3/ZrO_2 [6-10]. Al_2O_3/YAG eutectic crystal has a homogeneous 'Chinese script' lamellar structure. Growth of these materials in fiber form yields an improvement in the mechanical properties [5] because the fiber crystals have a very high strength due to their crystalline perfection and small dimensions. The eutectic microstructures depended on the growth speed, and the interlamellar spacing of the eutectic microstructures has an inverse-square-root relation to the growth rate [11].

In this article, the fiber growing of Al_2O_3/YAG, Al_2O_3/ZrO_2 binary and Al_2O_3/YAG/ZrO_2 ternary eutectic systems has been carried out using the micro-pulling down (below abbreated as μ-PD) technique, and their microstructures and preliminary mechanical properties

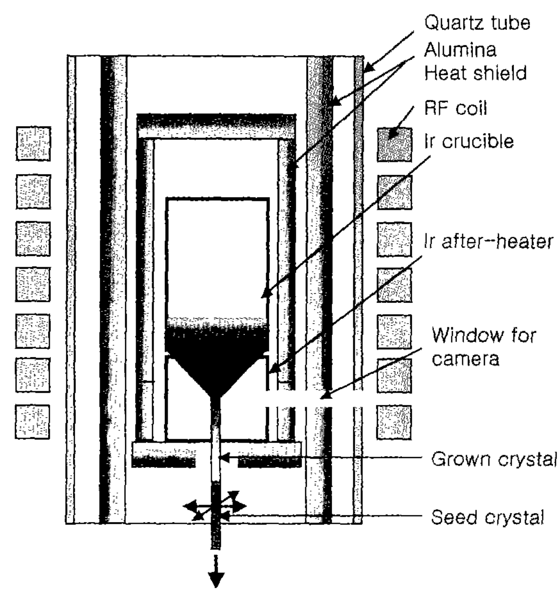

Fig. 1. Schematics of micro-pulling down apparatus.

†Corresponding author
Tel: 81-22-215-2102
Fax: 81-22-215-2104
E-mail: jholee@imr.edu

have been studied comparatively as a function of solidification rate.

2. Experimental Procedure

The μ-PD apparatus used in this study consisted of an iridium crucible coupled with an RF induction heating module, a cylindrical iridium after-heater, and appropriate thermal insulation, as described in Fig. 1. The conical crucible bottom had a central capillary hole about 0.3 mm in diameter and 1 mm in length. A sapphire [0001] fiber crystal was used as a seed. The meniscus and growing crystal were observed by CCD camera. The growth was performed under flowing Ar gas atmosphere to prevent from the oxidation of Ir crucible and after-heater. The growth process was controlled by manual adjustment of RF power and pulling rate.

4N-purity of Al_2O_3 (High-Purity Chemical Co.), Y_2O_3 (Nippon Yttrium Co.) and ZrO_2 (Rare Metallic Co.) were used for the starting materials. As shown in Fig. 2, there is only one eutectic point in Al_2O_3-YAG and Al_2O_3-ZrO_2 binary systems, and their melting tempera-

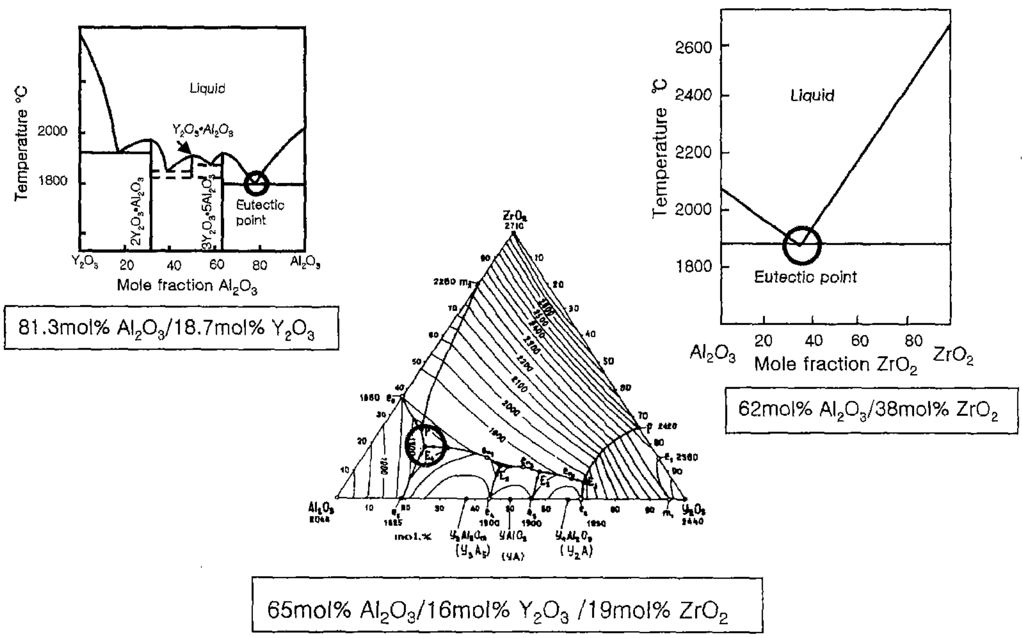

Fig. 2. Phase diagrams for the Al_2O_3-based eutectic systems used in this study.

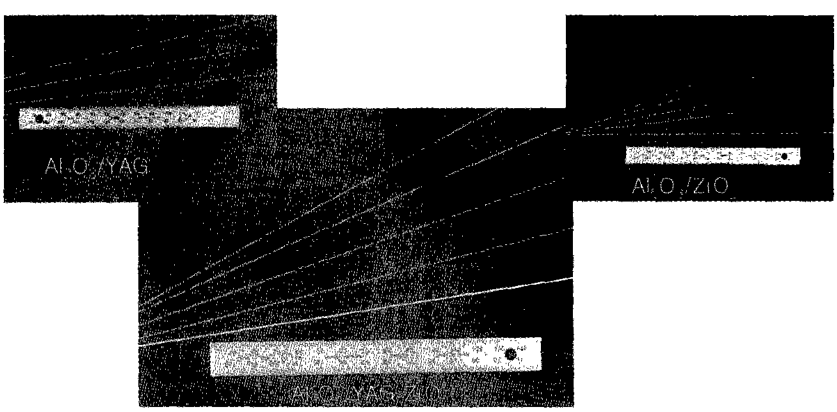

Fig. 3. As-grown Al_2O_3-based binary and ternary eutectic fibers.

tures are 1830°C and 1870°C respectively. However, several eutectic compositions were reported in the ternary eutectic system of Al_2O_3, Y_2O_3 and ZrO_2, but only one point is for the Al_2O_3, YAG and ZrO_2 ternary system which is placed on the 65 mol% Al_2O_3, 19 mol% ZrO_2 and 16 mol% Y_2O_3, and its melting temperature is 1715°C [14]. Then, starting materials were mixed to binary and ternary eutectic composition of Al_2O_3/YAG, Al_2O_3/ZrO_2 and Al_2O_3/YAG/ZrO_2. In the case of Al_2O_3/ ZrO_2, it was doped 1~9 mol% of Y_2O_3 as a stabilizing agent for zirconia.

Eutectic fibers of 0.3~2.0 mm diameter and up to 500 mm in length were grown over the range of pulling rate of 0.1~15 mm/min.

The eutectic fibers grown at various pulling rates were characterized by scanning electron microscope (SEM) and energy dispersive spectroscopy (EDS) to identify the eutectic microstructure and chemical compositions. Microstructure images were obtained from both perpendicular and longitudinal polished sections to the growth direction using the back-scattered emission (BE) mode of the SEM. The intercellular spacings were evaluated on the chosen line on the perpendicular cross section to the growth direction.

To investigate mechanical properties of the grown eutectic fibers, we examined the tensile strength using a universal testing machine (UTM) with crosshead speed of 0.1 mm/min at room temperature in air and high temperatures of 800, 1200 and 1500°C in vacuum.

3. Results and Discussion

As-grown Al_2O_3-based eutectic fibers had near nearly white color as shown in Fig. 3. Stable growth was obtained in the range of 0.1~15 mm/min. It was possible to control the fiber diameter from approximately 0.3 mm to 2 mm within 10 % of diameter stability. The maximum length was about 500 mm, limited by the apparatus.

Figure 4 shows a powder XRD pattern of crushed Al_2O_3-based YAG, ZrO_2 binary and ternary eutectic fibers. All phases were composed of crystalline alumina, YAG and zirconia. There was no trace of other phases such as $Y_4Al_2O_9$ (Y_2A) or $YAlO_3$ (YA) in Al_2O_3/ YAG and Al_2O_3/YAG/ZrO_2 eutectic systems, but peaks of the cubic zirconia phase were shifted slightly as some amount of Y_2O_3 was dissolved. In Al_2O_3/ZrO_2 eutectics, it can observe that these eutectic fibers were composed of only two phases of alumina and zirconia, and there were no traces of the other phases such as YAG. Dominant zirconia phases in undoped and low content of Y_2O_3 below 1 mol% had the monoclinc form, but in a higher content over 3 mol%, the monoclinic changed to cubic phase via a tetragonal one. On the basis of qualitative results under EDS, some amount of Y_2O_3 was contained in the ZrO_2 phase. For the solubility limit of Y_2O_3 in ZrO_2, Echigoya [13] reported 13.3 mol%, but Lakiza [12] wrote 19.2 mol%.

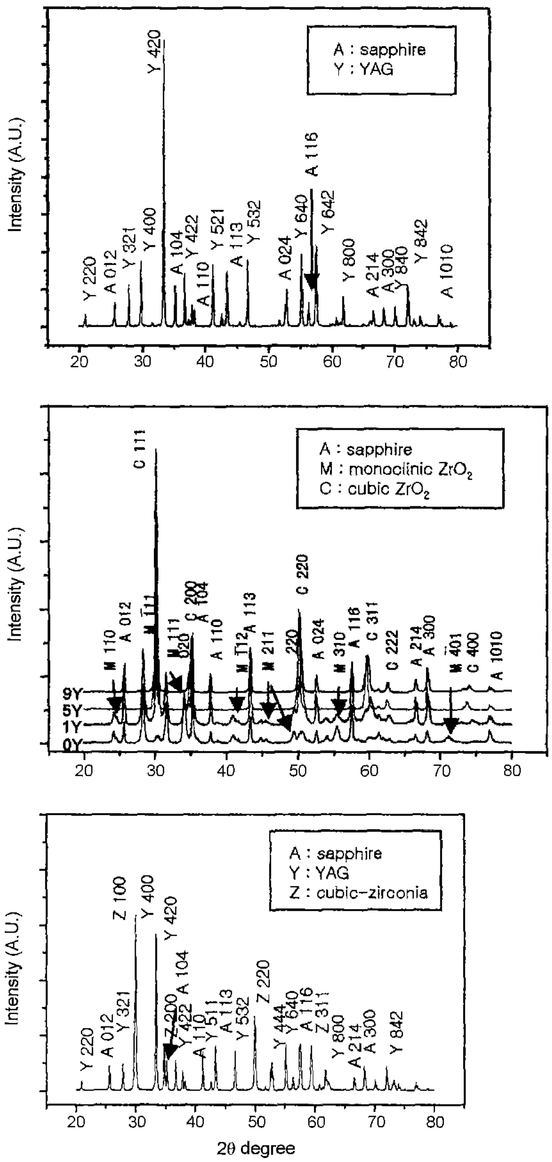

Fig. 4. Powder XRD pattern of crushed Al_2O_3-based eutectic fibers.

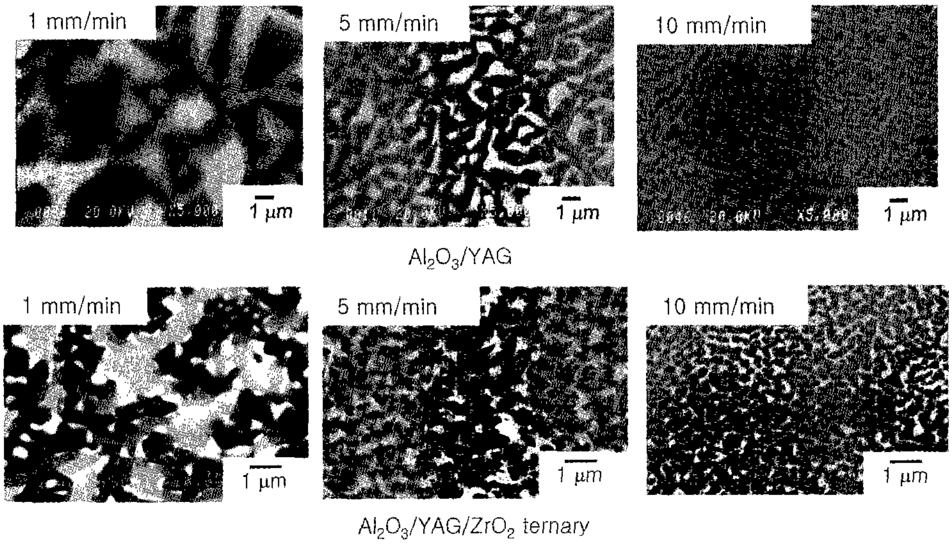

Fig. 5. SEM images of perpendicular cross-section of Al_2O_3/YAG binary and Al_2O_3/YAG/ZrO_2 ternary eutectic fibers grown at various pulling rates, 1 mm/min, 5 mm/min and 10 mm/min.

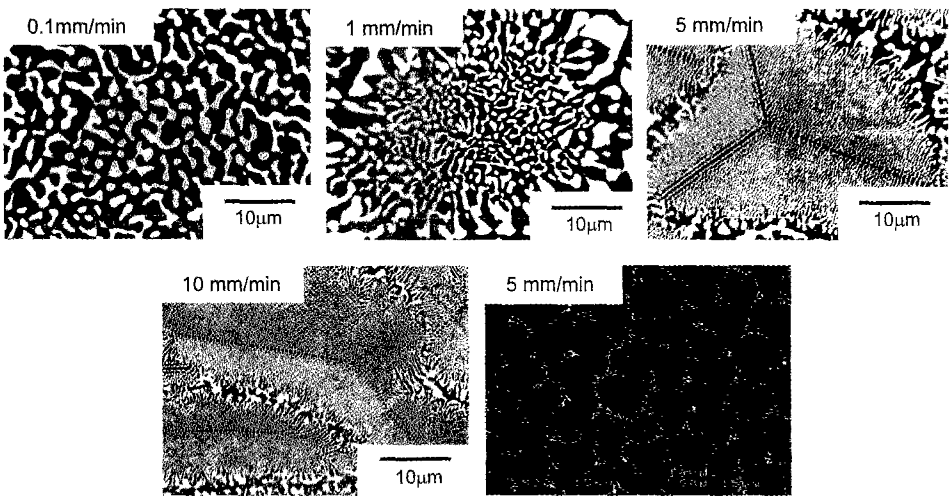

Fig. 6. SEM images of perpendicular cross-sections of Al_2O_3/ZrO_2 (Y_2O_3) binary eutectic fibers grown at the pulling rate of 0.1 mm/min, 1 mm/min, 5 mm/min and 10 mm/min.

Although quantification of dissolved Y_2O_3 was not carried out in this work, it was clear that a small amount of Y_2O_3 dissolved in the ZrO_2 phase.

Typical eutectic microstructures were shown in Figs. 5 and 6 as a function of solidification rate. The eutectic microstructures were composed of two or three phases depending on the eutectic component, and distinguished by their different shapes and colors. By EDS analysis, the black matrix was shown to be Al_2O_3, and the white phases were YAG or ZrO_2 in binary systems in these studies. While the eutectics containing YAG showed homogeneous 'Chinese script' lamellar pattern like Fig. 5, the microstructure of Al_2O_3/ZrO_2 binary eutectics changed from lamellar structure to cellular-lamellar pattern via circular and triangular colony structure with the solidification rate as shown in Fig. 6.

In the ternary eutectics, gray YAG phase made a homogeneous second phase on the black sapphire matrix, and the ZrO_2 phases were distributed on the periphery of the YAG phase as relatively small particles that appear white in the micrograph. Both YAG

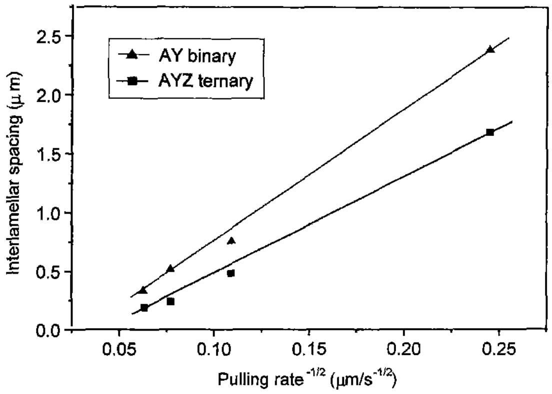

Fig. 7. Interlamellar spacing versus solidification rate of Al_2O_3-based eutectic fibers.

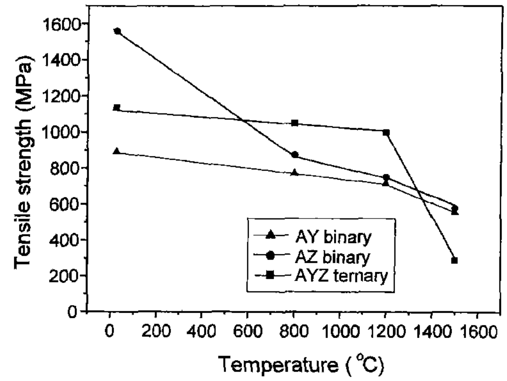

Fig. 9. High temperature tensile strength of Al_2O_3-based binary and ternary eutectic fibers at the various temperatures.

and ZrO_2 phases in the ternary eutectics showed different morphologies compared to those of respective Al_2O_3-based binary eutectic systems. It could be observed that neighboring YAG grains were connected to each other, but the ZrO_2 particles were scattered.

In all the eutectic system studied, the microstructure changed its size with solidification rate. In the eutectics containing YAG, the interlamellar spacing decreased from 2.4 to 0.5 and from 1.7 μm to 200 nm in the binary and ternary system respectively, as the pulling rate increased from 1mm/min to 15 mm/min, as plotted in Fig. 7. The general relation $\lambda \sim v^{-1/2}$ for the interlamellar spacing to solidification rate, where λ is the interlamellar spacing and v is the solidification rate, could also be applied successfully to the script structure of Al_2O_3-based YAG, ZrO_2 binary and ternary eutectics. The proportionality constants are close to 10 in binary and 8 in ternary, if λ is in mm and v is in μm/s.

SEM images of longitudinal cross-section in Fig. 8 showed that the script structure of the ternary eutectic connected three-dimensionally in both of microstructures developed at both low and high growth rate.

In order to examine the mechanical properties of the Al_2O_3-based YAG, ZrO_2 eutectic fibers, tensile strength tests were carried out the eutectic fibers grown at a pulling rate of 15 mm/min. As shown in Fig. 9, Al_2O_3/ZrO_2 binary eutectic fibers showed the highest strength of approximately 1560 MPa at room temperature, but their strength decreased drastically from 800°C. On the contrary, Al_2O_3/YAG/ZrO_2 ternary eutectic fibers recorded 1100 MPa at room temperature; the strength diminished only slightly with temperature until it decreased drastically to 280 MPa at 1500°C, due to the proximity of its melting temperature. The measured strength of Al_2O_3/YAG/ZrO_2 ter-

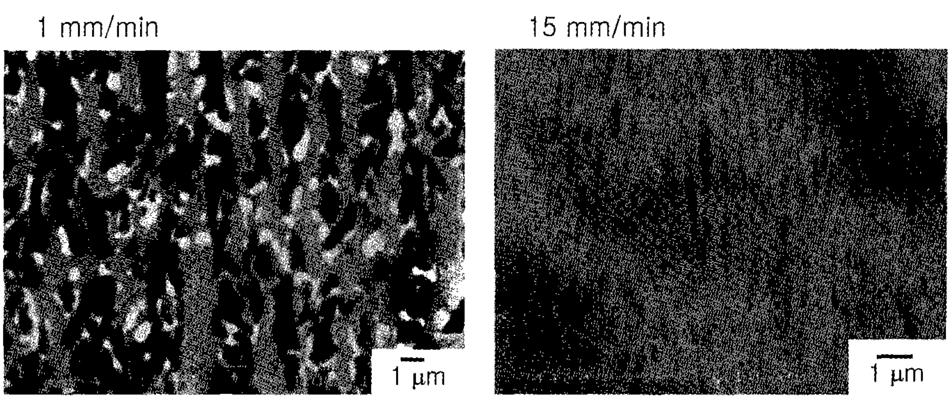

Fig. 8. SEM images of longitudinal cross-sections of Al_2O_3/YAG/ZrO_2 ternary eutectic fibers grown at the pulling rate of 1 mm/min, 15 mm/min.

nary eutectic fibers are much higher than the Al_2O_3/YAG binary one over the whole range of tested temperature except for 1500°C. It is assumed that higher strength of the ternary eutectic fibers over Al_2O_3/YAG results from both the strengthening effect of ZrO_2 and the smaller script size.

4. Conclusions

It was possible to grow the Al_2O_3 based YAG, ZrO_2 binary and ternary eutectic fibers using micro-pulling down method. While Al_2O_3/ZrO_2 showed cellular-lamellar structure, Al_2O_3/YAG and Al_2O_3/YAG/ZrO_2 ternary eutectic fibers showed homogeneous 'Chinese script' lamellar structures. The microstructure of Al_2O_3/ZrO_2 binary eutectic fibers changed with solidification rate from lamellar pattern to cellular structure.

The interlamellar spacing agreed with the inverse-square-root dependence on pulling rate according to $\lambda = kv_p^{-1/2}$. Al_2O_3/ZrO_2 binary eutectic fibers recorded the highest tensile strength of about 1560 MPa at room temperature. Al_2O_3/YAG/ZrO_2 ternary eutectic fiber showed excellent thermal stability up to 1200°C without significant decrease in tensile strength. The maximum recorded values were 1100 MPa at 25°C and 970 MPa at 1200°C, respectively.

References

[1] Y. Waku, N. Nakagawa, T. Wakamoto, H. Ohtsubo, K. Shimizu and Y. Kohtoku, Nature 389 (1997) 49.
[2] T.A. Parthasarathy, T.Y. Mah and L.E. Matson, J. Am. Ceram. Soc. 76 (1993) 29.
[3] Y. Waku, H. Ohtsubo, N. Nakagawa and Y. Koutoku, J. Mater. Sci. 31 (1996) 4663.
[4] Y. Waku, N. Nakagawa, H. Ohtsubo, Y. Ohsora and Y. Kohtoku, J. Jpn. Inst. Met. 59 (1995) 71.
[5] A. Yoshikawa, B.M. Epelbaum, T. Fukuda, K. Suzuki and Y. Waku, Jpn. J. Appl. Phys. 38 (1999) L55.
[6] F. Schmid and D. Viechnicki, J. Mater. Sci. 5 (1970) 470.
[7] S. Bourban, N. Karapatis, H. Hopmann and W. Kurz, Acta Mater. 45 (1997) 5069.
[8] T. Ando and Y. Shiohara, J. Am. Ceram. Soc. 74 (1991) 410.
[9] G.R. Fischer, L.J. Manfredo, R.N. McNally and R.C. Doman, J. Mater. Sci. 16 (1981) 3447.
[10] J. Echigoya, Y. Takabayashi, H. Suto and M. Ishigame, J. Mater.Sci. Lett. 5 (1986) 150.
[11] B.M. Epelbaum, A. Yoshikawa, K. Shimamura, T. Fukuda, K. Suzuki and Y. Waku, J. Crystal Growth 198/199 (1999) 471.
[12] S.M. Lakiza and L.M. Lopato, J. Am. Ceram. Soc. 80 (1997) 893.
[13] J. Echigoya, Y. Takabayashi, K. Sasaki, S. Hayashi and H. Suto, Trans. Jpn. Ins. Metals 27 (1986) 102.